QUASI-INSTANTANEOUS TWO-DIMENSIONAL TEMPERATURE MEASUREMENTS IN A SPARK IGNITION ENGINE USING 2-LINE ATOMIC FLUORESCENCE

C. F. KAMINSKI, J. ENGSTRÖM AND M. ALDÉN

Division of Combustion Physics
Lund Institute of Technology
P.O. Box 118
S-22100 Lund, Sweden

Two-dimensional thermometry by the two-line atomic fluorescence method (TLAF) from atomic indium performed in an internal combustion engine is reported for the first time. The engine was a modified production engine running on iso-octane fuel. Small quantities of atomized indium were admitted to the engine chamber by injecting solutions containing $InCl_3$ mixed with iso-octane. Temperatures could be measured over the entire combustion cycle covering a range from 800 to 2800 K at pressures up to 14 bar. A precision of 14% on single-shot temperature distributions was obtained, a figure that is expected to be much improved if laser intensity profile normalization is performed on a shot-by-shot basis and not, as in the present case, on averaged intensity profiles. Advantages of the technique are its sensitivity over a large temperature range, its insensitivity to collisional quenching processes, the small laser powers required, and the possibility to use wavelengths at which interferences from native flame species, such as small hydrocarbons, are low. Limitations are discussed, and comparisons with other techniques are made.

Introduction

Data on temperature field distributions of turbulent combustion processes can provide important input for the improvement of theoretical models and the optimization of practical combustion devices. The task of measuring time-resolved temperature field distributions of burned gases is experimentally challenging, and few techniques are currently available that accomplish this task. Rayleigh and Raman scattering techniques using pulsed lasers have been applied to this end, but their low sensitivities make their use limited for two-dimensional temperature measurements of burned gases on a shot-by-shot basis [1]. Planar laser-induced fluorescence (PLIF), on the other hand, has the required sensitivity, and its application for single-shot thermometry has been demonstrated on molecular species such as OH [2] and NO [3]. These experiments are extensions of the two-line fluorescence methods reported in Refs. [4] and [5].

In two-line atomic fluorescence (TLAF), two temperature-sensitive electronic states in thermal equilibrium with the combustion gas are probed directly with two laser pulses. The ratio of the resulting fluorescence is proportional to the temperature. TLAF from metal species seeded into laminar flames has been shown to provide both accurate and precise temperature measurements with a precision reaching 2% on a shot noise basis [6,7]. More recently, point measurements of temperatures in turbulent flames were reported using continuous wave lasers modulated at frequencies up to 10 kHz and atomic indium as seeder species [8]. The precision of the technique was better than 3%.

A related technique is thermally assisted LIF [9], where collisional redistribution during the laser pulse length among states close to the laser-excited state results in fluorescence lines other than the one initially excited. If the system reaches thermal equilibrium, a temperature can be determined from the ratio of the spectrally resolved fluorescence line intensities. An advantage over TLAF is that only a single laser is required. Recently, thermally assisted LIF has been demonstrated to be capable of highly precise two-dimensional temperature measurements in flames [10]. However, owing to signal limitations, only time-averaged temperature measurements of laminar combustion events could be performed using thermally assisted LIF. Two-dimensional, single-shot temperature measurements using TLAF, on the other hand, have recently been demonstrated in flames seeded with atomic indium [11]. The present paper reports on the first application of this technique in a near-production SI engine running on iso-octane fuel. Burned gas temperature distributions could be measured on a shot-by-shot basis over practically the entire combustion cycle, with temperatures varying by ~2000 K. Advantages of the technique are presented as well as limitations, and comparisons are made with other laser thermometry methods.

Theory

The theory of TLAF is described in detail elsewhere [12]. Briefly, two time-delayed laser pulses at wavelengths λ_{02} and λ_{12} are used to probe the ground state 0 and first excited state 1 of a suitable seeder species by driving transitions to a common upper state 2. Upon excitation by λ_{02}, level 2 will fluoresce back to the two available lower states 0 and 1, yielding LIF signals F_{20} and F_{21}, respectively. A detector D_1 is used that is filtered to collect the LIF signal corresponding to F_{21} only. Similarly, another filtered detector D_0 collects the LIF signal F_{20} induced by λ_{21}. Because λ_{20} is degenerate with the signal wavelength F_{20} (and similarly λ_{21} coincides spectrally with F_{21}), time gating of the detectors must be used to discriminate against laser stray light. In turbulent combustion environments, the delay between the two excitation pulses must be chosen to be short on turbulent timescales but long enough for the population dynamics to relax to equilibrium before the second pulse arrives.

In thermal equilibrium, the ratio F_{20}/F_{21} can be directly related to the temperature T of the system. It can be shown that

$$T = \frac{\varepsilon_{01}/k_B}{4 \ln \frac{\lambda_{21}}{\lambda_{20}} + \ln \frac{I_{12}}{I_{02}} + \ln \frac{F_{21}}{F_{20}} + C} \quad (1)$$

where ε_{01} is the energy difference between the two lower states involved (in J), k_B is Boltzmann's constant, λ_{2i} are the fluorescence wavelengths, and I_{i2} and F_{2i} $(i = 0, 1)$ are the laser and the fluorescence signal intensities, respectively. C is a system-dependent calibration constant that needs to be determined separately and includes factors such as spectral overlap between laser and atomic linewidths, detector and light collection efficiencies, etc., and is best determined by performing a calibration measurement in a system with known temperature. Equation 1 is valid under the assumption of a linear relationship between laser intensity and LIF signal. Because the oscillator strengths of atomic seeder species can be of the order of unity, the effects of saturation and fluorescence trapping have to be carefully checked for in a given measurement situation. Note that because F_{21} and F_{20} usually correspond to very different frequencies in TLAF and because the populations in the lower two states are different, the amount of signal trapping will not be equal for the two signals. This is in contrast to some molecular two-line techniques where due to fast collisional redistributions, the spectral shapes of the fluorescence may be very similar for the two excited lines [4]. In the present case, saturation and self-absorption must be checked for by establishing so-called curves of growth [13] for different laser intensities and seeder species concentrations.

The large spin orbit splitting ε_{01} in the ground state of many metal atoms makes them ideally suited as seeder species for TLAF thermometry because the population distribution over states 0 and 1 can be sensitive over a large range of temperatures [11,13]. In the present case, atomic indium was chosen because it offers good sensitivity in a T range encountered in a multitude of practical combustion environments ($\sim$500–3000 K). The large oscillator strengths of metal species as seeds means that only minute quantities and small laser powers are required, an advantage for PLIF applications.

The measurement error of the temperature evaluated from the TLAF signals will be a combination of errors from F_{20} and F_{21} and laser intensity measurements. It can be written as

$$\frac{\sigma_T}{T} = \frac{Tk_B}{\varepsilon_{01}} \left[\left(\frac{\sigma_{F_{21}}}{F_{21}} \right)^2 + \left(\frac{\sigma_{I_{02}}}{I_{02}} \right)^2 + \left(\frac{\sigma_{F_{20}}}{F_{20}} \right)^2 + \left(\frac{\sigma_{I_{12}}}{I_{12}} \right)^2 \right]^{1/2}$$

$$(2)$$

where σ_x/x denotes the relative error in the quantity x. Furthermore, shifts in temperature will result from errors in the calibration constant C in equation 1.

Experiment

Engine

Figure 1 shows a schematic diagram of the engine used in the experiments. The engine top was a research version of the Volvo N1P engine fitted onto an AVL 528 one-cylinder engine, equipped with an AVL 514 optical access option. Laser access was either through quartz pentroof windows, allowing probing close to valves and spark plug, or through a 30-mm quartz liner to allow measurements further down into the chamber. The direction of the laser beams was perpendicular to the plane of Fig. 1. LIF signals propagating through the transparent piston were reflected out of the engine block by a 45° mirror prior to detection by the camera system. All measurements reported in the present paper correspond to the 5-mm measurement position in Figure 1.

To obtain maximal reproducibility, the fuel and air were premixed by injecting the fuel into a heated, 2-m-long pipe, which ensured complete vaporization of the charge, prior to entry into the combustion chamber. To reduce the amount of residuals in the combustion chamber from previous engine cycles, the system was run on skip-fired mode, with ignition occurring every fifth cycle only. Cycle-to-cycle variations of cylinder pressure and heat release were kept below 10% in this way [14]. The engine characteristics and present operating conditions are detailed in Ref. [14].

Optical Setup

A Spectra-Physics PIV 400 double-cavity Nd:YAG laser was used to pump the two dye lasers (Lumonics
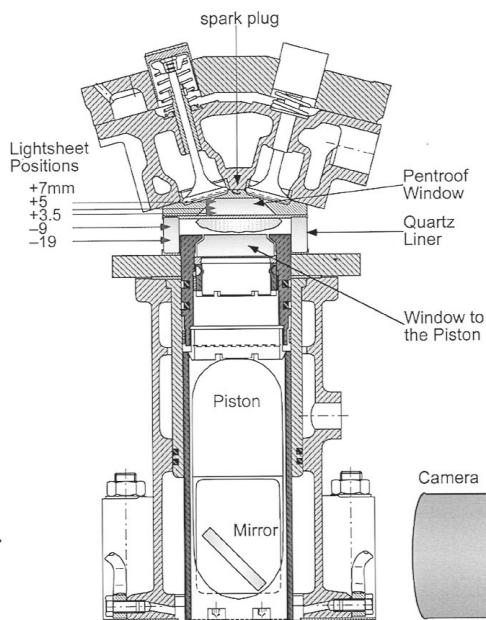
FIG. 1. Optical access to the engine chamber. A 45-degree mirror placed below the transparent piston was used to reflect the TLAF signals out of the chamber.

Hyperdye-300) used in the present experiments. The frequency-tripled output at 355 nm from cavity 1 was used to pump dye laser 1 operating on methanol solutions of Coumarin 445 to obtain output at 451 nm. Pulses from cavity 2 were delayed by 500 ns with respect to cavity 1 and frequency doubled to 532 nm. This was used to pump a dye laser at 667 nm whose output was subsequently mixed with the residual fundamental radiation at 1064 nm to provide output around 410 nm. The beams were spatially filtered and attenuated and formed into sheets of approximately 200 μm thickness and 6 cm width. Pulse energies were approximately 80 μJ per pulse in the interaction region and monitored on a shot-by-shot basis by use of a fast photodiode and two boxcar-integrating amplifiers (Stanford SRS250). Care was taken to sample the same spatial extent of the beams as entered the reaction chamber.

TLAF signals were monitored by two intensified CCD cameras (LaVision Flamestar II) with 14-bit dynamic resolution and a chip size of 576 by 384 pixels. Both cameras were equipped with standard 105-mm camera lenses (Nikon). A beamsplitter coated to be highly reflecting at 45° for F_{21} and highly transmitting for F_{20} was used to separate the optical axes for the two signals. The two detecting cameras were arranged at right angles to each other and mounted on precision x, y, z, θ positioning stages. Combined with software mirroring of one of the camera images, this allowed precise alignment

of the two images on a pixel-by-pixel basis. The light collection solid angle of the imaging system was maximized corresponding to ~f/9 for the given engine geometry and signal path. Distortions caused by the intensifiers (cushioning, misalignment of fiber couplers, etc.) were undetectable on the present image scale, and no further software image corrections had to be employed once alignment had been achieved.

Trigger pulses for the whole system were derived from a crankshaft encoder that was referenced to the fuel injection pulse provided by the AVL electronics. At 1200 rpm, this corresponded to a pulse train at 10 Hz to which the YAG lasers could be synchronized, which were optimized for this repetition rate. Cameras were triggered only every fifth cycle, when ignition occurred. Separate pulses were provided for YAG flashlamps, Q switches, interpulse delay, camera intensifier gates, and CCD exposure, achieved by the use of three delay generators. In this way, the TLAF system could be locked to any desired crank angle.

Seeding Procedure

InCl$_3$ salt was dissolved in a few droplets of isopropanol and then mixed with isooctane at typical concentrations of 700 μg mL^{-1}. The resulting solution was seeded into the heated premixing chamber by use of a spray atomizer assembly and a droplet size selector (Perkin Elmer). The doped isooctane was seeded at approximately 4 mL min^{-1}, and the rest of the fuel–air mixture was injected via a standard port injector into the premixing chamber. The combined air–fuel ratio was held stoichiometric.

Initial experiments were carried out by adding InCl$_3$ directly to the fuel and simply injecting it through the port injector, but for some reason, very low TLAF signals were obtained in this way, even at high seed concentrations. This is in contrast to earlier findings [11]. In the present case, fuel from the main tank was filtered before injection, and it is thought possible that the metal ions in solution underwent chemical changes upon filter passage, thereby reducing the amount of active species available in the cylinder chamber.

Reference Measurements

Laser sheet profile measurements were carried out using LIF from biacetyl added to the chamber just prior to and after each experimental run. Because sheet corrections were not performed on a shot-by-shot basis, fluctuations and long-term drifts in the beam profiles during measurement runs contributed to errors in the determination of T.

Background images were taken before and after each measurement series by triggering on a skipped cycle, where no ignition occurred and hence no

TLAF signal was measurable (see Results and Discussion).

Temperature references were obtained both before and after each measurement series by use of an acetylene-air flame, seeded by the same spray atomizer as used for the engine measurements. The burner nozzle consisted of a 4-mm inner diameter copper tube; gases were premixed stoichiometrically, which resulted in a very stable laminar flame. Prior to each measurement series, the engine top was removed and the burner nozzle was aligned for the flame to be intersected by the laser sheets. The flame temperature under these conditions had been determined previously using N_2 vibrational CARS measurements.

Results and Discussion

Extensive investigations—similar in nature to those reported in Ref. [8]—of laser absorption and fluorescence trapping behavior were carried out in laboratory acetylene-air flames using the same seeding apparatus as used for the engine measurements reported here. In these measurements, deviations from linearity occurred at seed concentrations above $600 \ \mu g \ mL^{-1}$ $InCl_3$ dissolved in water (at a seeding rate of $4 \ mL \ min^{-1}$, stoichiometric flame conditions). Under these operating conditions and laser intensities below saturation, signal levels were large enough to allow single-shot two-dimensional thermometry [signal-to-noise ratios (SNR) around 50:1 for F_{21} and 30:1 for F_{20} for single-shot images at flame temperatures]. TLAF signals varied linearly with laser pulse energy up to 80 μJ in the atmospheric pressure flame (0.2×60 mm sheet cross-sectional area), and for all measurements in the engine, energies were kept below this value.

Of course, these measurements could only serve as a guide for the engine measurements because the amount of TLAF active analyte present in the combustion system depends on a large number of parameters (combustor geometry that can affect the amount of laser and signal absorption, prevailing temperatures, concentrations of oxygen and other species that can react with indium, the type of solvent used in the seeding solution, and others that affect the seeding efficiency). For each given situation, therefore, the curve of growth yields the maximum permissible concentrations and laser intensities resulting in an optimal signal-to-noise ratio without compromising linearity. Under the present case, maximum signal levels were obtained around 351° crank angle (330° ignition) for the two lines. A growth curve was established at this crank-angle position corresponding to the average of 50 images each for different seed concentrations.

Up to concentrations of $700 \ \mu g \ mL^{-1}$, no deviations from linearity could be observed. This suggests that despite the dissimilarities between the two combustion systems (flame and engine), similar amounts of active analyte are produced in the measurement region if the atomizer was operated under similar conditions. It should be noted at this point that the advantage of the large oscillator strength of atomic species resulting in strong signal levels is offset by the demand to keep concentrations below the limit where significant trapping or laser absorption results and maximum signal-to-noise levels are not expected to be larger than if molecular species are used. One has, however, the advantage of being able to control the amount of active species present via the seeding mechanism, which is of course not possible with native species.

Figure 2 shows mean temperature distributions obtained for various crank-angle positions for the engine running under the conditions described in Ref. [14] (measurement height 5 mm). Each image corresponds to the average of 30 single-shot temperature distributions obtained at each particular crank angle. The first picture in the series indicates the section of the chamber seen by the cameras, intake valves are visible on the left, exhaust gas valves to the right. The spark plug is situated in the center, a pressure transducer is seen in the top section of the picture.

For each individual image pair obtained from the cameras, T was calculated on a pixel-by-pixel basis. Averaged background images were subtracted from each individual picture. The biacetyl reference images described earlier were averaged and binned along the direction of the laser beam. The profiles thus obtained were normalized to one and the TLAF images divided by this profile to account for intensity variations across the laser sheet. The images were then processed according to equation 1 on a pixel-by-pixel basis subject to the condition that intensities were larger than 40 counts for both signals. The remaining pixels were not used in the temperature evaluation. This signal-to-noise criterion was balanced to minimize noise on calculated temperatures on the one hand and maximize the range of temperatures that could be measured in the engine. If the cut-off is chosen too high, regions of cold temperatures where F_{20} is low cannot be measured, and biasing toward higher T could result. In the present case, temperatures as low as 800 K could be measured late in the cycle. The point at which this bias occurred was determined by an iterative procedure that increased the cut-off value until temperature distributions late in the cycle began to change in the way described. The T distributions shown are binned to 192 by 288 pixels and compressed to 10 grayscale levels to aid visualization.

The error in the fluorescence ratio $R = F_{21}/F_{20}$ is directly reflected in the error of T. Late in the cycle, where T is low, this error is mostly due to shot noise in F_{20}. An estimate of the shot noise can be made
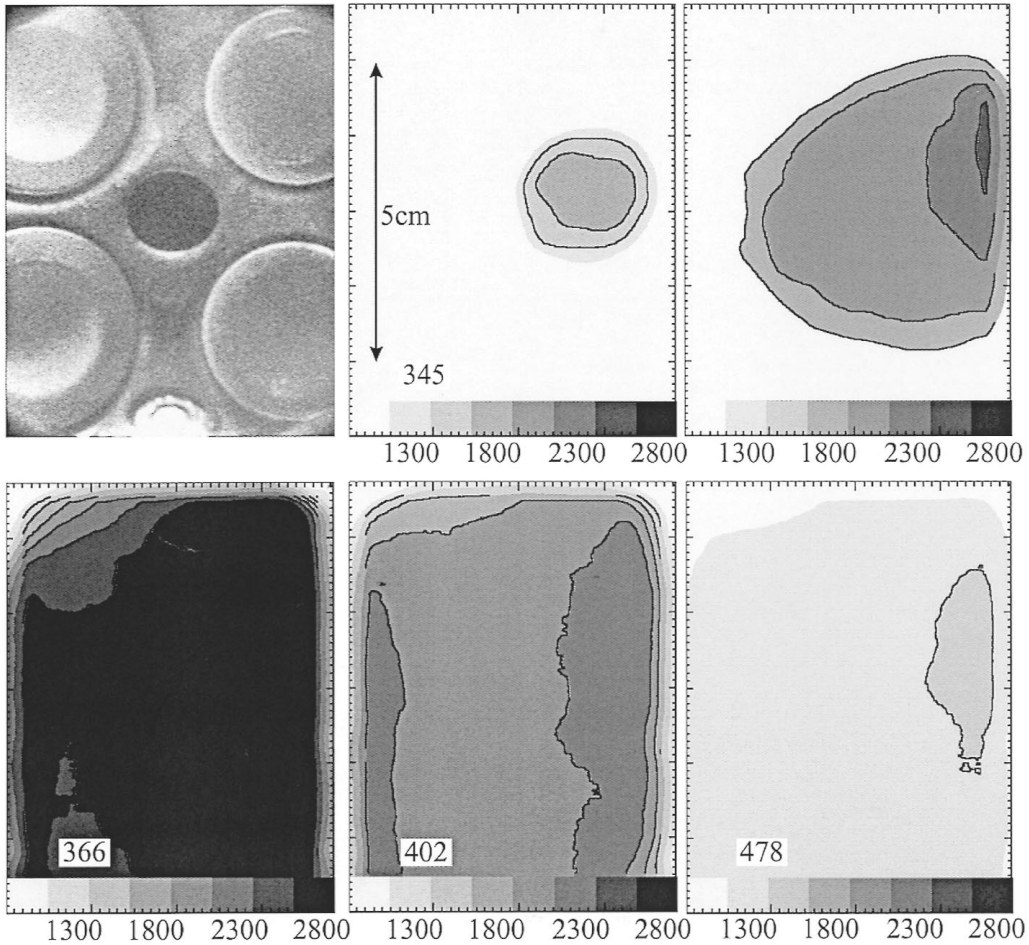
FIG. 2. Averages of 30 single-shot T-distributions. Crank angle positions (degrees c.a.) are indicated in the lower left-hand corner of respective diagrams. The first picture in the series shows the field of view of the two cameras. Intake valves are to the left, exhaust valves on the right. The spark plug is situated in the center of the figure. A pressure sensor is situated near the top of the figure. The temperature scales are in K.

following the method described in Ref. [12]. Assuming a maximum error in R of 10% late in the cycle, an error of 3% is obtained at 800 K. The error resulting from time-averaged beam profile referencing can be estimated from the standard deviation of single-shot biacetyl fluorescence profiles from the mean profile. Standard deviations were of the order of 9%, and this introduces a maximal error of 7% at the maximum T measured in the present case (2800 K). Shot-by-shot referencing of the sheet profile using, for example, a linear diode array could improve this imprecision. It has been suggested also [8] that laser mode noise can introduce substantial fluctuations in atomic LIF due to the small atomic absorption widths. Current investigations using a modeless dye laser [15] are aimed at measuring the effects of mode noise on TLAF signals. These and other laser

spectral properties will affect the calibration constant C in equation 1 over time and will affect the precision. Errors in the determination of the reference flame temperature will furthermore shift measured temperatures systematically. In total, the maximum error in calculated temperatures on single-shot temperature distributions is estimated to be 14% at a maximum temperature of 2800 K, a value that could be substantially improved if shot-by-shot laser profile referencing is performed.

The flame propagation can be clearly seen in the sequence shown in Fig. 2. After maximum pressure occurring near 368° c.a., the temperature distribution is essentially constant across the cylinder diameter and remains so until very late in the cycle. Early in the cycle (345° and 351° c.a.), the flame is seen to develop to the right-hand side of the viewing
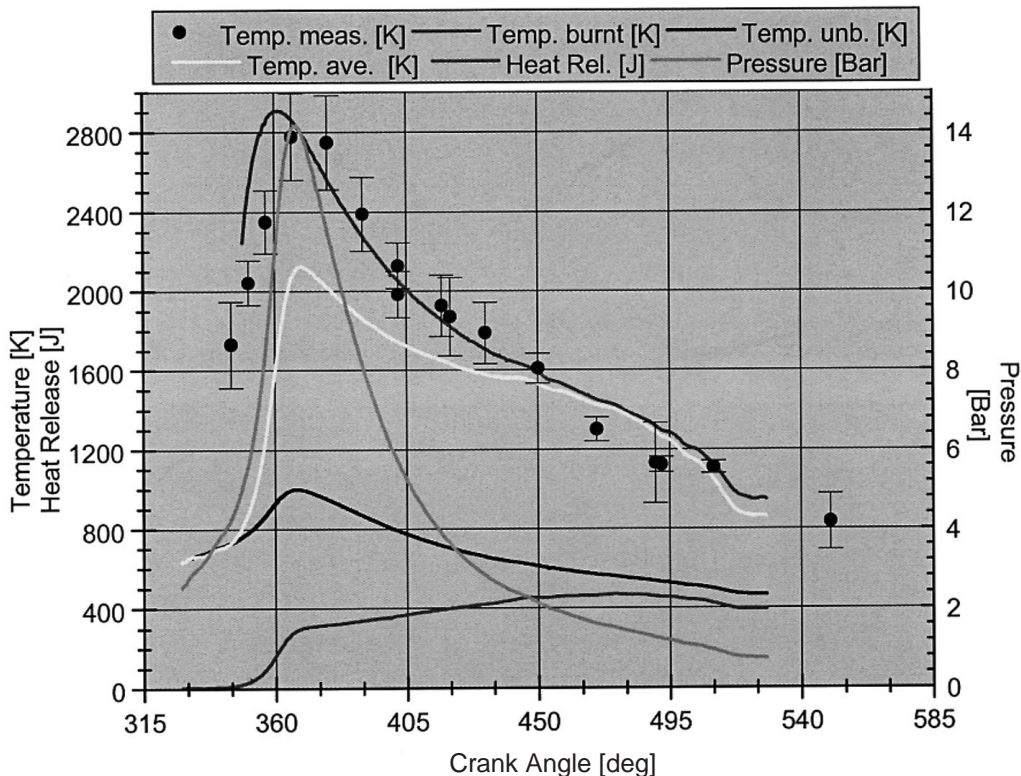
FIG. 3. Comparison of measured mean burnt temperatures as seen in Fig. 2 and calculated temperatures obtained from pressure data and thermodynamic analysis. The pressure curve and curves for unburned and averaged gas temperature, and the heat release are also shown.

field, which corresponds to the position of the exhaust gas valves. Particle image velocimetry (PIV) measurements of flow fields were performed in the present engine and are reported in Ref. [14]. The PIV measurements revealed a strong tumbling motion of the fuel charge toward the exhaust valves, which explains the observed phenomenon.

In Fig. 3, the averages of evaluated temperature distributions such as in seen in Fig. 2 are shown. The graph corresponds to the averaged burned gas temperatures. Error bars correspond to the standard deviation of single-shot mean temperatures from the average temperature (shown as solid circles). Also shown on the graph is a pressure trace from which the solid gas temperature curves and the heat-release curve shown were calculated using engine thermodynamic analysis [14]. From the graph, the large T range that can be measured with the present technique is evident, spanning a range of around 2000 K. The initial rise of T early in the cycle seems to under-represent the curve calculated from the pressure data. A possible explanation is given later.

An extensive database of T data from the present

measurements is being generated corresponding to a variety of engine operating conditions and measurement positions. It will be used as input for detailed numerical simulations of gasoline engine combustion. In particular, it is currently being used for validation of models for NO_x formation and emission in conjunction with measurements of NO concentration in the same engine under similar conditions [14].

Examples for single-shot T distributions are shown in Figure 4, corresponding to 345° c.a. Cycle-to-cycle variations of the flame development in the engine are clearly visible on these images, and this demonstrates the great advantage of two-dimensional thermometry techniques over point measurements. In a given point, the temperature may change by hundreds of Kelvins, from shot to shot. In contrast to the present technique, point measurements yield no information about the cause of such changes (e.g., changes of flame location, misfiring, etc.), and the results are correspondingly more difficult to interpret. Averaged over 30 shots, T distributions, as in Fig. 4, yield distributions such as shown in Fig. 3 for
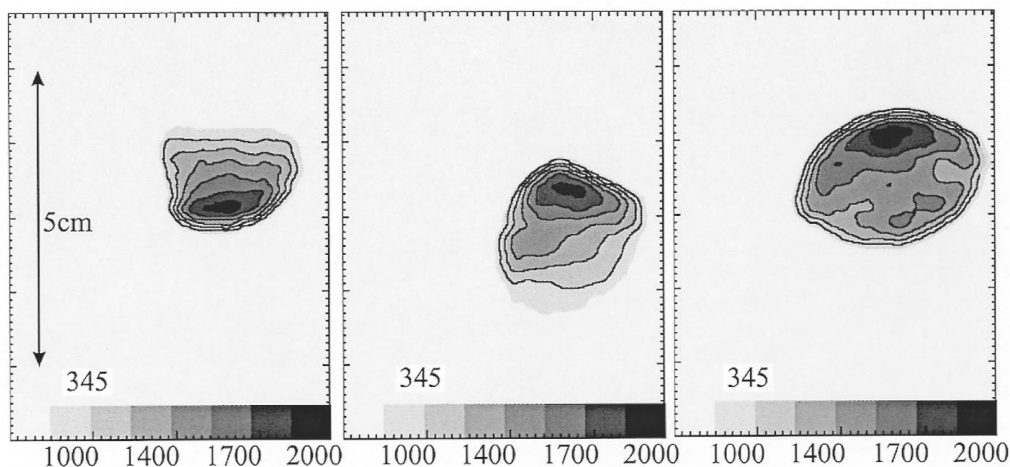
FIG. 4. Single-shot temperature distributions corresponding to 345° c.a. Cycle-to-cycle variations resulting in fluctuations of the flame location are clearly visible.

345° c.a. The change in flame location reduces the averaged flame temperature. Because the experimental data in Fig. 2 is based on averaged data, this may explain why measured Ts appear lower early in the cycle than the calculations based on the pressure data. Figure 4 clearly demonstrates the feasibility of single-shot thermometry with the present technique.

In contrast to OH two-line thermometry, the technique is capable of monitoring the entire combustion cycle. The enormous T dependence of OH production during combustion means that only a small range of crank angles early in the cycle can be measured. Toward maximum temperatures, the OH content increases dramatically, and strong absorption influences measurement precision. The rapid fall of T after maximum pressure means signal-to-noise ratios soon become too small for single-shot thermometry. The amount of active indium, on the other hand, is nearly constant throughout the combustion cycle (although oxidization may occur, reducing the amount of neutral indium), with signal levels essentially only influenced by temperature-induced population changes between the lower two levels. Despite the changing optical path length during each cycle (because of piston movement), this means also that the amount of signal trapping is nearly constant as a function of crank angle because the total number of absorbers stays constant.

A disadvantage of the present technique is of course the seeding requirement with a foreign species (which is, furthermore, toxic). The presence of metal atoms may change the radical balance in the combustion process via three-body collisions. This can affect, for example, the relative abundance of H and OH radicals, although the effect is minute for indium at the present concentrations. The TLAF

process is effected by a combination of solvent vaporization, species volatilization, and subsequent atomization by electron-ion recombination, to produce the TLAF active species. Alkemade [16] has estimated the influence of such processes on flame temperature for seeding conditions similar to what is presented here. In general, it was found that these effects are negligible in comparison to the chemical energy released during combustion (combined effect less than a percent in the present case). An exception to this is the heat consumed during evaporation of the solvent, which in some circumstances can lead to significant cooling of the flame. However, because in the present case the fuel was used directly as the solvent and vaporized in the premixing chamber, such cooling effects are not relevant for the present application.

As seen, the present technique is limited to measuring the burned gas temperature because neutral indium is formed only in the presence of a flame via electron-ion recombination or molecular dissociation. Before ignition, therefore, despite the relatively high temperatures established during compression, no TLAF signal can be observed at all. In the case of nonreactive high-temperature flows, two-line PLIF thermometry using NO as seeder species has been applied successfully [3]. On the other hand, the severe sensitivity of NO to collisional quenching, which affects position and shape of observed transitions, makes its application to reactive flows very difficult.

Two-dimensional, time-resolved Rayleigh thermometry of combustion events has been reported in the past. A disadvantage is that Rayleigh cross sections are widely varying for different species, and this makes data evaluation very difficult in complex

environments such as SI engines. Furthermore, very large laser powers are required that can perturb the flame chemistry.

One of the most distinct advantages of the indium–TLAF method is that only minute laser powers are required and excitation and fluorescence occur in the visible wavelength region where absorption by small hydrocarbons and other native species in combustion is small. This is in contrast to the other techniques discussed earlier, which are performed in the UV spectral region. Current experiments are carried out in sooting flames and engines running on commercial fuels to investigate the potential of TLAF in these environments.

Conclusion

Time-resolved, two-dimensional thermometry of highly turbulent combustion events has been demonstrated for the first time using two-line atomic fluorescence (TLAF). The technique was applied successfully to a near-production automotive engine running on isooctane fuel. The temperature sensitivity of the technique allowed measurements over the entire combustion cycle to be performed covering a temperature range of nearly 2000 K. The technique is conceptually simple and should find applications in a variety of hot, reacting flows.

REFERENCES

1. Eckbreth, A. C., *Laser Diagnostics for Combustion Temperature and Species,* 2nd ed., Combustion Science and Technology Series, vol. 3, Gordon and Breach Publishers, New York, 1996.
2. Seitzman, J. M., Hanson, R. K., DeBarber, P. A., and Hess, C. F., *Appl. Opt.* 33:4000–4012 (1994).
3. MCMillin, B. K., Palmer, J. L., and Hanson, R. K., *Appl. Opt.* 32:7533–7545 (1993).
4. Cattolica, R., *Appl. Opt.* 20:1156–1166 (1981).
5. Lucht, R. P., Laurendeau, N. M., and Sweeney, D. W., *Appl. Opt.* 21:3729–3735 (1982).
6. Omenetto, N., Benetti, P., and Rossi, G., *Spectrochim. Acta* 27B:453–461 (1972).
7. Bradshaw, J., Nikdel, S., Reeves, R., Bower, J., Omenetto, N., and Wineefordner, J. D., in *Laser Probes for Combustion Chemistry* (D. R. Crosley, ed.), ACS Symposium Series 134, American Chemical Society, 1980, pp. 199–203.
8. Dec, J. and Keller, J. O., in *Twenty-First Symposium (International) on Combustion,* The Combustion Institute, Pittsburgh, 1986, pp. 1737–1745.
9. Elder, M. L., Zizak, G., Bolton, D., Hovath, J. J., and Winefordner, J. D., *Appl. Spectrosc.* 38:113–118 (1984).
10. Berten, H. O. and Kleinermanns, K., *Appl. Phys. B* 61:605–610 (1995).
11. Kaminski, C. F., Engström, J., and Aldén, M., *VDI Berichte* 1313:555–560 (1997).
12. Alkemade, C. T. J., *Pure Appl. Chem.* 23:73–97 (1970).
13. Haraguchi, H., Smith, H., Weeks, S., Johnson, D. J., and Winefordner, J. D., *Appl. Spectr.* 31:156–163 (1977).
14. Hildenbrand, F., Schulz, C., Sick, V., Josefsson, G., Magnusson, I., Andersson, Ö., and Aldén, M., *SAE paper* 980148 (1998).
15. Ewart, P., *Opt. Commun.* 55:124 (1985).
16. Alkemade, C. T. J., in *Flame Emission and Atomic Absorption Spectrometry,* vol. 1 (J. A. Dean and T. C. Rains, eds.), Marcel Dekker, New York, 1969, pp. 100–151.

COMMENTS

Michael Drake, General Motors, USA. Can this measurement technique be used to measure end gas temperatures in IC engines? Specifically, have you tried to make measurements close to surfaces, and are there problems? Second, can you seed with indium compounds that are less thermally stable than indium chloride that you used in the present experiments? This could lead to dissociation in the end gas providing the atomic indium in the end gas needed for your technique.

Author's Reply. I presume this question is related to knock studies in engines. With the present technique, we have been unsuccessful in getting TLAF signals from indium before ignition. There are other indium compounds that are less stable than $InCl_3$, for example, metal-organic compounds, but many are very toxic or otherwise difficult to handle. I believe that in our case, an electron ion recombination is required in the gas phase before neutral indium is produced, and the flame enhances this process. Possibly, use of a vapor of pure indium or a compound that produces atomic indium when dissociated can be used for this purpose. Concerning the question of measurements near engine walls, we have not tried this yet. In the present application, there was no evidence of contamination of the cylinder walls by indium, but if low wall temperatures prevail, loss of indium by condensation and consequent loss of signal may pose a problem.

•

Yasuo Takagi, Nissan Motor, Japan. In the single-shot temperature distribution data, the temperature in the peripheral region of the flame looks too low (about 1000 K). Can you comment why?

Author's Reply. The one-sided temperature gradients on single-shot temperature distributions were only visible very early in the cycle. The measurements shown correspond to a short time period after ignition, where the flame kernel had just reached the region we were probing with our laser sheet. The effect was changing from shot to shot. I assume it is caused by turbulent gas flow onto the developing flame kernel, which initially propagates at low speeds. In this context, the gradients could be explained by transport of hot flame gases out of the flame via turbulent diffusion.